Quantitative Biology 2022, 10(3): 264–275
https://doi.org/10.15302/J-QB-021-0275

RESEARCH ARTICLE

Scale-adaptive superpixels for medical images

Limin Sun, Dongyang Ma, Yuanfeng Zhou*

School of Software, Shandong University, Jinan 250100, China
* Correspondence: yfzhou@sdu.edu.cn

Received January 31, 2021; Revised March 5, 2021; Accepted March 11, 2021

***Background*: Superpixel segmentation is a powerful preprocessing tool to reduce the complexity of image processing. Traditionally, size uniformity is one of the significant features of superpixels. However, in medical images, in which subjects scale varies greatly and background areas are often flat, size uniformity rarely conforms to the varying content. To obtain the fewest superpixels with retaining important details, the size of superpixel should be chosen carefully.**

***Methods*: We propose a scale-adaptive superpixel algorithm relaxing the size-uniformity criterion for medical images, especially pathological images. A new path-based distance measure and superpixel region growing schema allow our algorithm to generate superpixels with different scales according to the complexity of image content, that is smaller (larger) superpixels in color-riching areas (flat areas).**

***Results*: The proposed superpixel algorithm can generate superpixels with boundary adherence, insensitive to noise, and with extremely big sizes and extremely small sizes on one image. The number of superpixels is much smaller than size-uniformly superpixel algorithms while retaining more details of images.**

***Conclusion*: With the proposed algorithm, the choice of superpixel size is automatic, which frees the user from the predicament of setting suitable superpixel size for a given application. The results on the nuclear dataset show that the proposed superpixel algorithm superior to the respective state-of-the-art algorithms on both quantitative and quantitative comparisons.**

Keywords: superpixels; scale adaptive; medical images; segmentation

Author summary: Most superpixel algorithms help reduce the complexity of image processing by generating superpixels with uniform size and boundary adherence. For freeing the users from the predicament of setting suitable superpixel size for a given application, and taking account of the multi-scale of different tissues in medical images, we propose a scale-adaptive superpixel algorithm for medical images, generating superpixels with multi-scale according to the complexity of image content. As demonstrated by the experimental results, our method is superior to other superpixel methods for medical images segmentation.

INTRODUCTION

Superpixel segmentation, a kind of image over-segmentation technique, is a powerful preprocessing tool to reduce the complexity of image processing. Superpixel algorithms aggregate pixels with similar properties to form more representative areas so that the number of image processing primitives are reduced from millions of pixels to a few thousands of superpixels. Most of these small areas retain effective information for further image processing, generally the boundary information of the objects in image. Since first proposed by Ren and Malik [1], superpixel segmentation has been widely used in medical image processing, *e.g.*, tumor segmentation from multimodal MRI [2], superpixel-guided label softening [3], vessel segmentation and catheter detection in X-ray angiograms [4],

segmentation of breast ultrasound image [5], segmentation of large 3D medical datasets [6–8], and more others like [9, 10]. In order to facilitate processing of downstream tasks, superpixels often have the following properties [11, 12]: boundary adherence, uniform size, compactness and computational efficiency.

Depending on different usage, there are many kinds of medical images, computerized tomography (CT) images, magnetic resonance (MR) images, ultrasound (US) images, Digital pathology (DP) images [13] and so on. Medical images produced by particular imaging techniques, are very different from natural images. For instance, on CT or MR images, different tissues and organs have big differences in size and gray level in foreground area, by contrast, background areas are large and flat. The sizes of superpixels obtained by traditional superpixel method are basically similar, which does not take account of the multi-scale characteristics of medical images.

Traditional superpixel techniques can be divided into two categories: graph-based algorithm and non-graph-based algorithms. Graph-based methods model the foreground and background segmentation problem as the minimum cut problem of the graph. Normalized cuts algorithm (NCUTS) [14] is one of the earliest graph-based methods. Liu *et al*. [12] presented entropy rate superpixel (ERS) algorithm that connects subgraphs by maximizing the entropy rate of a random walk. Felzenszwalb and Huttenlocher [15] proposed a minimum spanning tree based segmentation algorithm (FH), which do not create uniform-size superpixels.

Most non-graph-based algorithms are gradient ascent methods, which focus on minimizing an energy function defined by a suitable distance measure. One of the most prominent superpixel algorithms is the Simple Linear Iterative

Clustering algorithm (SLIC) [16], a k-means clustering based algorithm. Simple non-iterative clustering (SNIC) [11] use a priority queue to generate superpixels in a non-iterative way. The turboPixels algorithm (TURBO) [17] uses the level set to compute the evolution of superpixels. Zhou *et al*. [18] defined bilateral geodesic distance (Bi-Geodesic) to generate superpixels with region compactness and region boundary regularity. SEEDS [19], a non-graph-based algorithm, iteratively evolves an initial rectangular approximation of superpixels using coarse to fine pixel exchanges with neighboring superpixels. The watershed algorithm (WSHED) [20] accumulates similar pixels starting from local minima to find lines that separate segments. The mean shift algorithm (MSHIFT) [21] iteratively locates local maxima of a density function and pixels that lead to the same local maximum belong to the same segment.

In recent years, deep network based superpixel algorithms appear. Superpixel sampling network (SSN) [22] develops a new differentiable model for superpixel segmentation that leverages deep networks to learn features for superpixel clustering via an end-to-end training framework. Yang *et al*. [23] present a novel method that employs a simple fully convolutional network to predict superpixels on a regular image grid, superpixel segmentation with fully convolutional networks (SSFCN). Both SSN and SSFCN generate superpixels with boundary adherence and uniform-size. More reviews of superpixel methods can refer to [24, 11].

SLIC, SNIC, TURBO, ERS and SEEDS allow the user control over the number of output superpixels. This property lets the user choose the size of the superpixels based on the needs. Most uniform-size superpixel algorithms are initialized with the grid-based seeding. This spatial constrain encourages uniform superpixel size but ignores the underlying image complexity or scale [25]. In other words, a major drawback of uniform size property is that it cannot perceive small scale targets that smaller than uniform superpixel size when the number of superpixels is small. When uniform superpixel size is small enough, the number of superpixels is increased heavily by dividing the large scale and homogeneous target into many superpixels. It can increase the complexity of image processing, as well can not counter the noise inside the large scale target.

There are several methods considering generating superpixels with controllable size, MSHIFT, FH, [25–28]. Achanta *et al*. [25] proposed a scale adaptive superpixel based on the local texture and scale of an image (Adaptel). Uziel *et al*. [26] proposed self-coined Bayesian adaptive superpixel segmentation (BASS), together with an efficient inference for adaptive superpixels. Refs. [25,26] are designed for natural images, without considering the characteristics of medical images. In [27], Bauchet and Lafarge can generate polygons with different sizes, but the size of the superpixels are not controllable. In [28], Ma *et al*. can generate convex polygons with controllable size by using features such as image boundary. But the superpixels generated by Refs. [27,28] are all polygons, which are not suitable for complex medical images.

Inspired by [25], we propose a new scale adaptive superpixel algorithm relaxing the size-uniformity criterion for medical images that over comes the abovementioned limitation. In [25], superpixels are grown sequentially to occupy an area and position constrained by an energy threshold *Th*. A superpixel is grown from a seed, and the neighbors of superpixel boundary pixels with smallest color difference to superpixel average color are added to superpixel, until

the color difference sum with all pixels in superpixel reaching threshold *Th*. In our method, superpixels are also generated sequentially. A superpixel area grows from a seed pixel making use of breadth-first search and a new greedily shortest path strategy. There is a path distance threshold that constrains the growth of superpixel.

Our contributions are as follows:

• Our algorithm can generate superpixels with different scales according to the richness of medical image content, that is smaller (larger) superpixels in color-riching areas (flat areas) (Fig. 1);

• A new path-based distance measure is proposed, making use of breadth-first search and greedily shortest path strategy;

• We employ a priority queue as distance comparing for computational efficiency, approaching real-time performance; Superpixels are generated sequentially, thus only one target superpixel in local areas in memory at one time, which requires less memory for large-size images.

Extensive experiments demonstrate that our algorithm performs outstandingly against the state-of-the-art methods in both quantitative validation as well as visual validation on medical images.

RESULTS

Our algorithm is implemented with Matlab. In order to demonstrate the advantages of the proposed superpixel segmentation method on medical images, we conducted experiments on pathological images [29, 30] and CT images [31], respectively. We have made qualitative comparison on datasets [29–31], qualitative comparison and quantitative comparison on dataset [29]. The dataset [29] consists of annotated H&E stained histology images captured at 40× magnification. The Ref. [29] contains 30 images 1000×1000 from seven different organs, with a total of 21,623 nuclei labeled. The dataset [30] is the pathological image data of cervical cells. The dataset [31] contains MRI images of the brains of 95 infants aged 0 to 1 years and is often used in medical image segmentation studies. In this section, we mainly compare the classical superpixel segmentation algorithms: NCut [14], TurboPixel [17], Bi-Geodesic [18], VCell [32], SEEDS [19], SLIC [16], BASS[26] and Adaptel [25]. We give the qualitative and quantitative comparisons of the experimental results. In the quantitative comparisons, the evaluation criteria commonly used in superpixel segmentation algorithms are used to evaluate the accuracy of various methods on medical image segmentation. In the qualitative comparisons, we present the results of our method and make a visual comparison with other methods.

Qualitative evaluations

In this part, we firstly give the visual comparison with other methods, and then give the superpixel results generated by our method under different thresholds.

Visual comparisons of our method against other methods

Figures 2 and 3 show visual comparisons of our method with other methods on pathological images in Refs. [29,30]. Multi-scale features are also evident in the cell image, for example, the area of the nuclear region is much smaller than the area of the cytoplasm. For this kind of image, the traditional methods often pay too much attention to the similarity of size and the regularity of shape, but ignore the scale diversity of various tissues in the pathological images. It can be seen from the

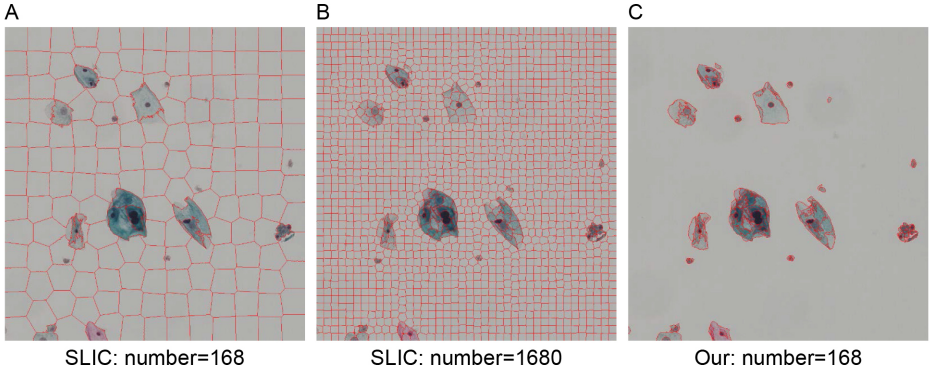

Figure 1. The predicament of choosing the right superpixel size. (A) and (C) have the same number of superpixels, and that of (B) is ten times of (A) and (C). For uniform-size superpixel segmentation, (B) retains detail but obtains too many superpixel, (A) lose structures smaller than the superpixel size, such as nuclear. With our scale-adaptive superpixels segmentation (C), the choice of size is automatic, and the number of superpixels is small while retaining detail of image.

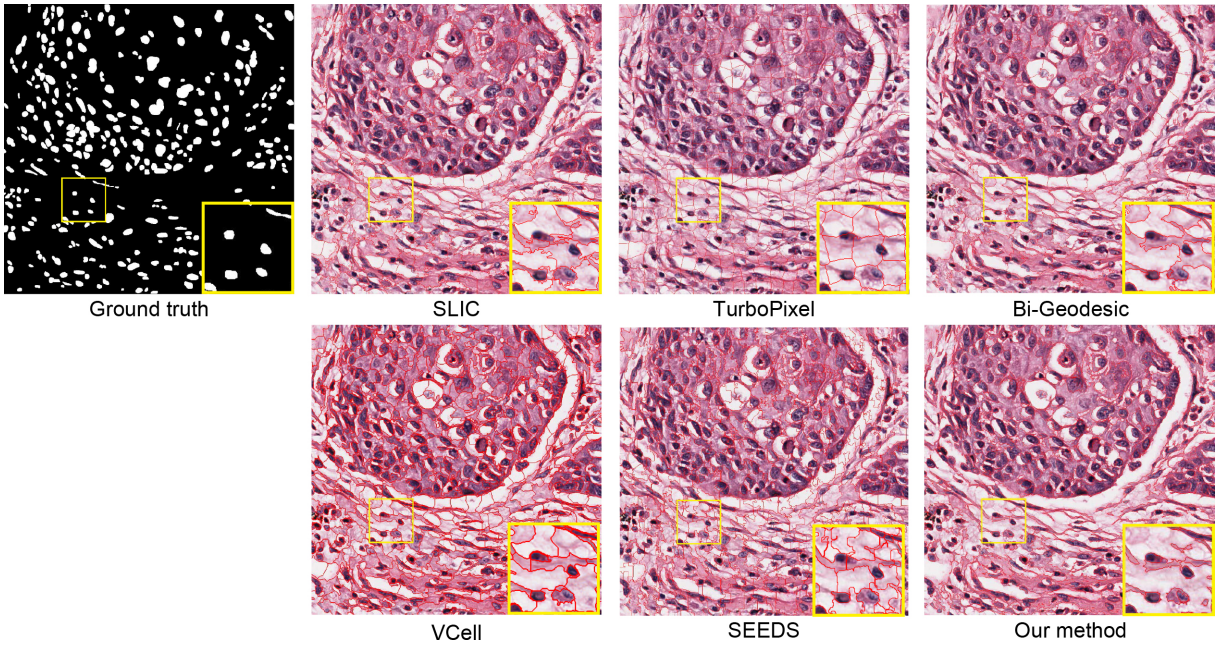

Figure 2. Visual comparison on histology images.

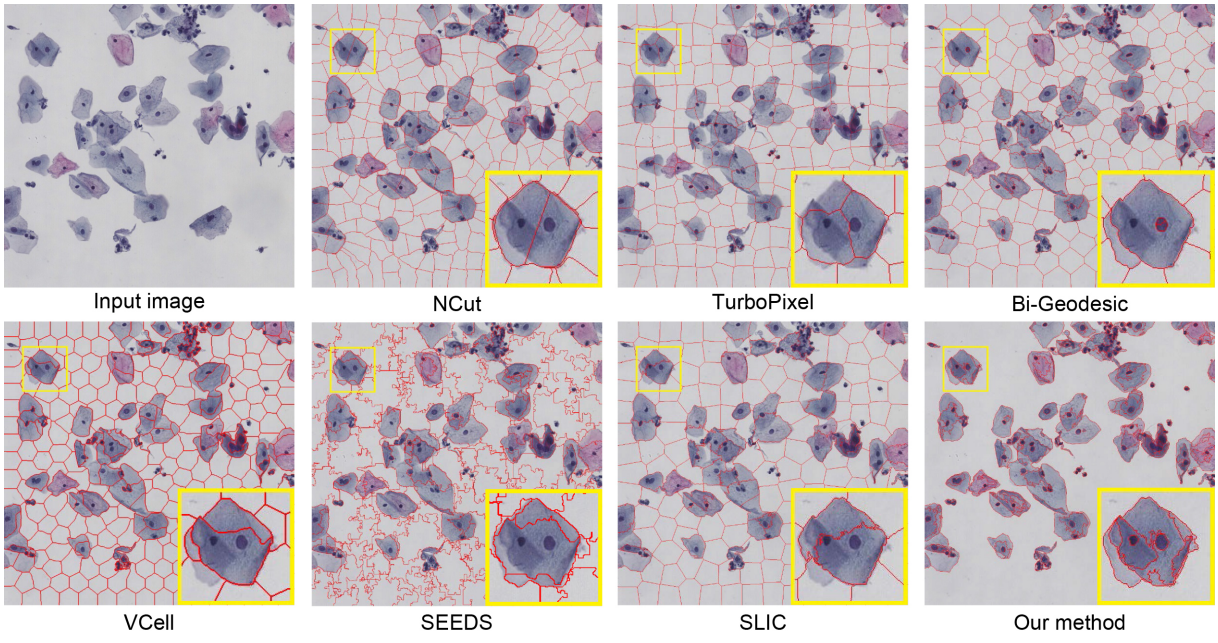

Figure 3. Visual comparison on cervical cell images.

results of visual comparison that our method can use a relatively large superpixel to segment the background region or the cytoplasmic region with a large area, and a relatively small superpixel to segment the nuclear region. We also deliberately compare our method with other scale adaptive superpixel methods BASS [26] and Adaptel [25]. We respectively compare the results when the number of superpixels is 500, 1100, and 1500. As shown in Fig.4, our results are significantly better than those of other methods.

In order to verify the effectiveness of our method, we also performed a visual comparison on CT images with other methods. Figure 5 shows a visual comparison of the results of our method and other methods on CT images. It can be seen from the Ground Truth that there is a large difference in the scale of each tissue. For

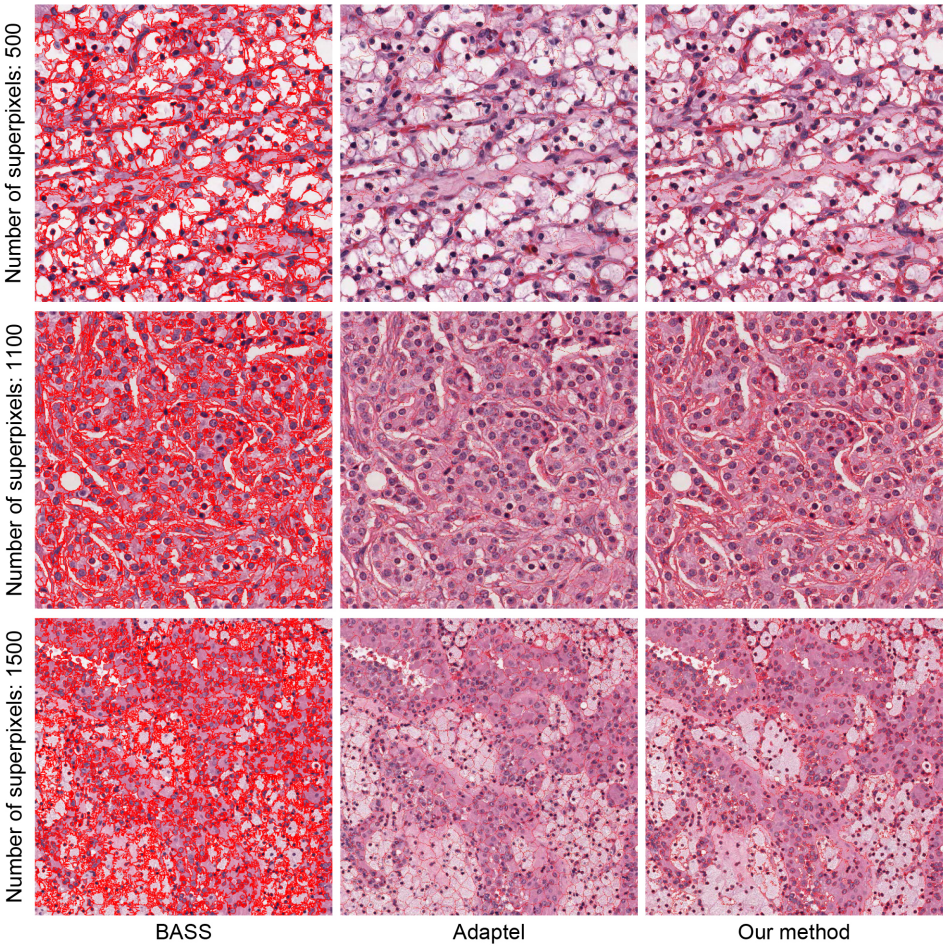

Figure 4. Visual comparison on histology images with scale adaptive superpixel methods.

example, the blue label has a large area, while the red label has a small and scattered area. The comparison of visual results shows that our method has advantages in processing this kind of CT data. From the region of interest (yellow box), it can be seen that our method can segment a tissue with a small number of superpixels and has a good boundary alignment.

Results under different β and threshold T

There are two important parameters, threshold T and parameter β, in our method. β and threshold T are described in detail in Section "MATERIALS AND METHODS". Next, we will focus on analyzing the influence of different β and threshold T on the experimental results. β mainly affects the maximum size and boundary alignment of superpixels, while T mainly affects the minimum size and number of superpixels. In general, for fixed T and fixed β, the number of superpixels generated will be different if the complexity of the image content is different. The more complex the image is, the more superpixels are generated.

Figure 6 shows the visual comparison under different values of β and threshold T. Parameter β is the weight of the second item, in the range of [0, 1]. The smaller β is, the smaller the influence of the color difference of other pixels is, the more pixels can a superpixel take in, the bigger the size of superpixel may be, the smaller the superpixel number is. The smaller β is, the bigger the influence of the difference of current processing pixel is, the better the boundary adherence is.

Threshold T constrains the max path distance. When the path distance of current processing pixel reaching threshold T, current processing pixel is assigned a boundary pixel of superpixel. The bigger threshold T is, the more pixels can a superpixel take in, the bigger the size of superpixel may be, the smaller the superpixel number is.

Quantitative evaluations

In order to evaluate the accuracy of superpixel results, we used the evaluation criteria: boundary recall (BR) [17],

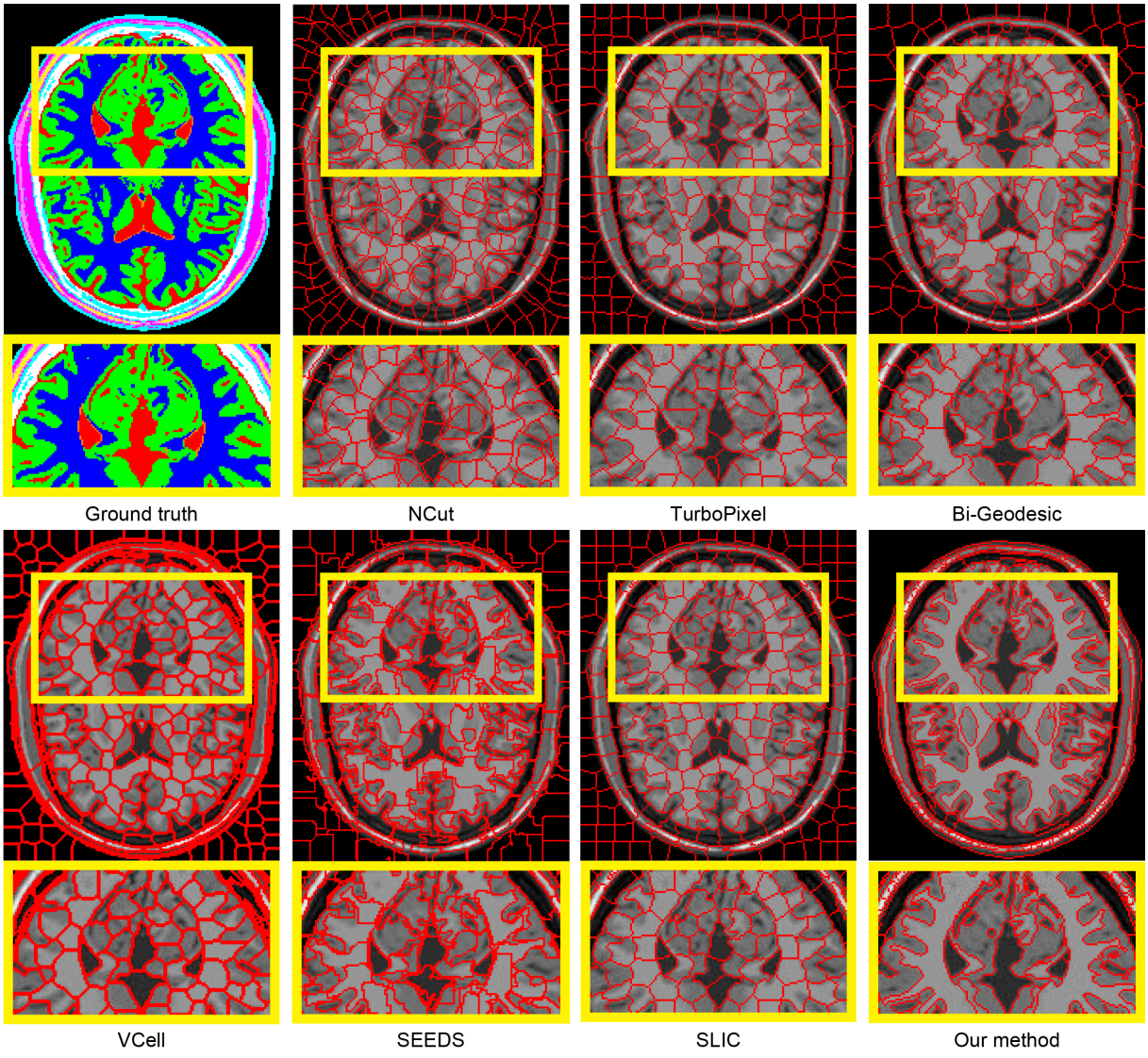

Figure 5. Visual comparison on CT images.

undersegmentation error (USE) [33], and achievable segmentation accuracy (ASA) [34].

$$BR = \frac{|SP \bigcap GP|}{|GP|}, \mu = 2, \tag{1}$$

where SP are pixels on boundaries generated by the superpixel segmentation, GP are pixels on ground truth boundaries, $|\cdot|$ represents the number of pixels, μ is disk-shaped neighborhood of the superpixels boundaries.

$$ASA = \frac{\sum_i \max_j |S_i \bigcap G_j|}{\sum_j |G_j|} \tag{2}$$

$$USE = \frac{1}{\sum_j |G_j|} \left[\sum_i \sum_j \min \left\{ S_i \bigcap G_j, S_i - G_j \right\} \right], \tag{3}$$

where S_i is a superpixel segmentation and G_j is a segmentation of the ground truth.

We made a quantitative comparison with other superpixel methods on dataset [29]. As can be seen from Fig. 7, the segmentation accuracy of our method is better than that of other methods.

To verify the effect of parameter β and threshold T, we fix one parameter and examine the effect of the other parameter on the experimental results on [29]. We have given the visualization results under different parameters β and T in Fig. 6, and here we have given the quantitative comparison results. The experimental results are shown in Tables 1 and 2.

Both Tables 1 and 2 confirm the effect of parameter β and threshold T as we discussed in Section "Results under different β and threshold T". Both parameter β and

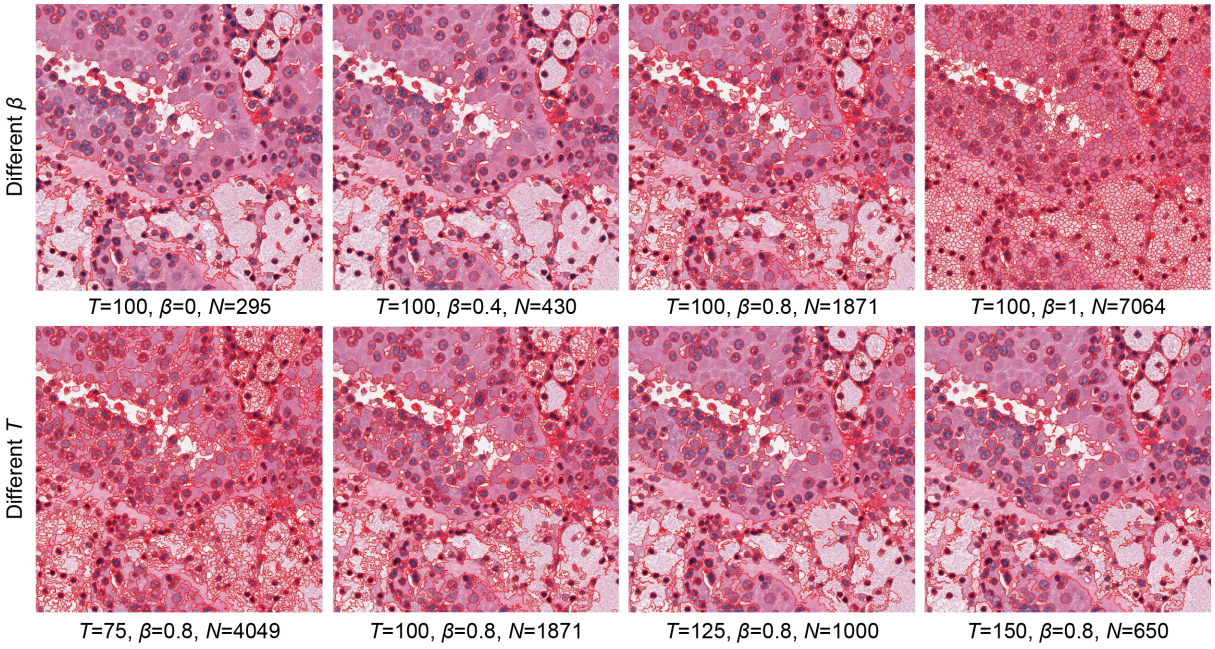

Figure 6. Results under different β and T. N represents the number of superpixels. Top: The results for different values of β. Bottom: The results for different values of T.

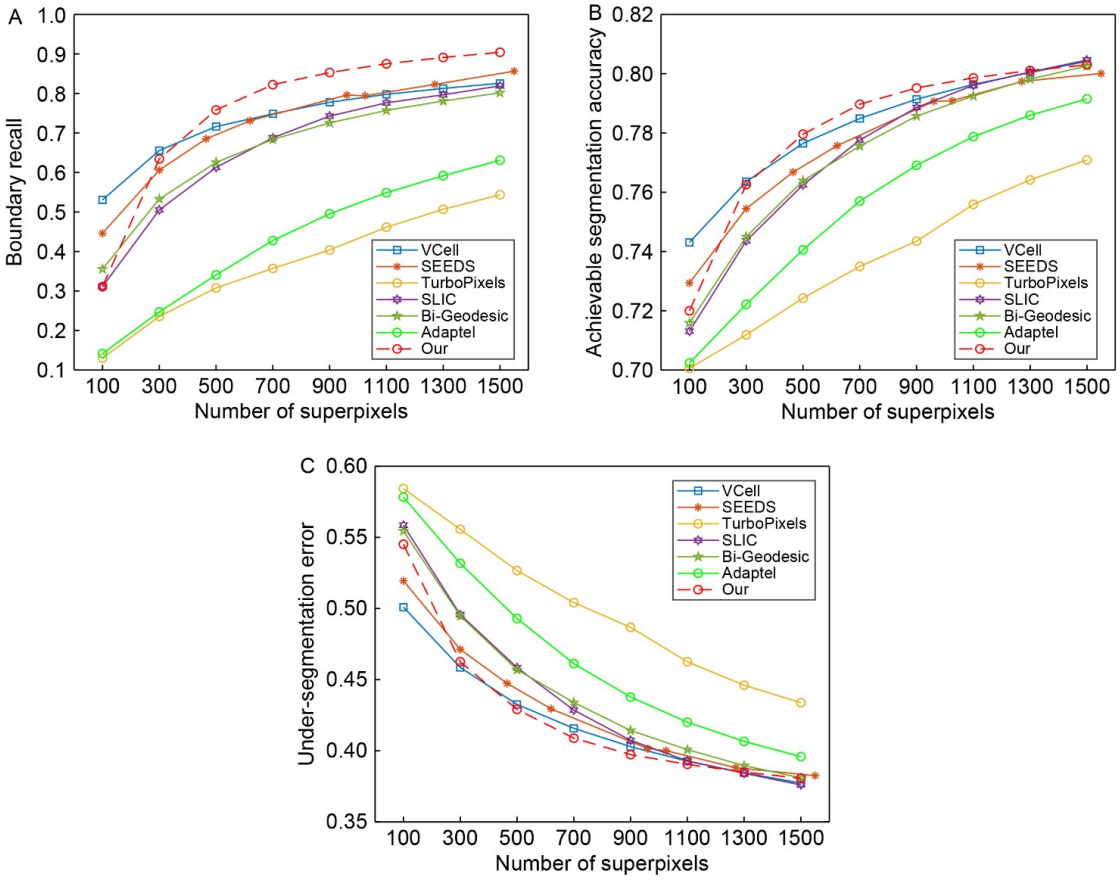

Figure 7. Experiments are performed on [29] to generate different numbers of superpixels by adjusting the desired number of superpixels. Parameter β is set 0.85. From left to right: *BR*, *ASA*, *USE*.

Table 1 Quantitative comparison on [29]

β	BR	ASA	USE	Average number
0.80	0.8670	0.7949	0.3981	1074
0.85	0.8958	0.8023	0.3824	1588
0.90	0.9221	0.8140	0.3568	3026
0.95	0.9405	0.8281	0.3271	6327
1.00	**0.9547**	**0.8343**	**0.3126**	9932

T=200, for different values of β.

Table 2 Quantitative comparison on [29]

T	BR	ASA	USE	Average number
50	**0.9931**	**0.8454**	**0.2897**	38434
100	0.9786	0.8299	0.3245	9905
150	0.9403	0.8141	0.3579	3434
200	0.8958	0.8023	0.3824	1588

β=0.85, for different values of T.

threshold T can influence the superpixel number. Empirically the boundary adherence increases when superpixel number increasing and there is a trade-off between superpixel number and boundary adherence. The recommended value range for β is [0.8,1].

DISCUSSION

Figure 7 show the quantitative evaluation results on the data published in [29]. The boundary recall (BR) curve of the proposed algorithm is significant higher comparing with the other five well-known superpixel algorithms. It convincingly proves that the proposed algorithm adheres best to object boundaries in ground truth. The undersegmentation error (USE) and achievable segmentation accuracy (ASA) are often quite similar for all superpixel algorithms. The proposed algorithm has the lowest error and highest accuracy in most cases. In general, the proposed method shows the best performance in quantitative validation.

Figures 3 and 5 show visual comparisons of the results of our method and other methods on pathological images and CT images, respectively. The results show that the proposed method can generate the most ideal superpixels and maintain the image boundaries better. In Fig. 3, our method segments nuclei most and get the highest accurate of cell boundary adherence. The number of background superpixels is just one to ten. One can easily separate cells and nuclei from background just depending on the superpixels sizes. This is the most direct evidence of the practicality of our method.

The current work is subjected to the following limitations since the parameters threshold T and β are defined by user. Firstly, parameter settings should be empirically selected. The complexity of medical images varies greatly between different types but less within a same type. Same parameters can be selected within a dataset of a same type. Secondly, the number of superpixels cannot be accurately estimated. The relationship among the threshold T, parameters β, the complexity of the image and the number of superpixels generated by the proposed algorithm should be explored later.

As the proposed method computes efficiently and almost real-time, it may be extended for high resolution images superpixel segmentation and extended to generate supervoxels for 3D image segmentation.

CONCLUSIONS

Superpixel segmentation have become a popular tool for image preprocessing. Each superpixel algorithm has its own advantages that suitable for particular applications. A novel scale-adaptive superpixel algorithm is proposed for medical images, which meets the appeal of superpixel size to obtain the fewest superpixels while keeping the most detail. The proposed superpixel algorithm can generate superpixels with extremely big sizes and extremely small sizes on the same image depending on the complexity of image content. This frees users from the predicament of setting the suitable superpixel size for a given application. The proposed method has the advantages, computational efficiency, tight boundary adherence, limited adjacency, insensitive to noise and multi-scale. Our method is simple to use and there is no need to set the superpixel size. We have verified our method on medical images, especially pathological images, and the experimental results show that our method is superior to other methods on medical images. It is trivial to extend the proposed algorithm to 3 dimensional data and this is a considerable work in the future.

MATERIALS AND METHODS

We propose a new scale adaptive superpixel algorithm relaxing the size-uniformity criterion for medical images. Superpixels are generated sequentially. A superpixel area increase from a seed pixel, making use of breadth-first search and greedily shortest path strategy, and an energy threshold defined by user constrain the growth of superpixel. A new path-based distance measure is proposed and we employ a priority queue as distance comparing for computational efficiency. The new distance measure and superpixel region growing scheme allow our algorithm to generate superpixels of different scales according to the complexity of image content, that is smaller (larger)

superpixels in visual complexity areas (flat areas) (Fig. 1).

Distance measure

Let C_k^t denotes the average color of the k^{th} superpixel S_k at time t, $|S| = t$.

Let $G = (V, E)$ denote an undirected graph consisted of n vertices $v \in V$ and m edges $e \in E \subseteq V \times V$ with cardinalities $n = |V|$ and $m = |E|$. Each pixel is associated with a vertex and locally connected to its 4 (or 8) neighbors. Let's assume there is a path P on graph G, $P = (p_0, p_1, p_2, ..., p_k)$, and $p_i (i = 0, ..., k)$ denotes the i^{th} point on the path P starting from p_0. The distance D_{p_i} of $p_i (i = 0, ..., k)$ is defined as follows:

$$
\begin{aligned}
&D_{p_0} = \text{colordis}_0 = 0;\\
&D_{p_1} = D_{p_0} \times \beta + \text{colordis}_1;\\
&D_{p_2} = D_{p_1} \times \beta + \text{colordis}_2;\\
&\quad \cdots\\
&D_{p_k} = D_{p_{k-1}} \times \beta + \text{colordis}_k\\
&\quad = \text{colordis}_0 \times \beta^k + \text{colordis}_1 \times \beta^{k-1} + \cdots +\\
&\quad \text{colordis}_i \times \beta^{k-i} + \cdots + \text{colordis}_k \times \beta^0\\
&\quad = \sum_{i=0}^{k} \text{colordis}_i \times \beta^{k-i}
\end{aligned}
$$

that is,

$$
D_{p_i} = \begin{cases} 0, & i = 0 \\ \sum_{i=1}^{k} \text{colordis}_i \times \beta^{k-i}, & i = 1, \ldots, k \end{cases} \tag{4}
$$

where $\text{colordis}_i (i = 1, ..., k)$, is the color distance between p_i and C_k^t, the average color of the k^{th} superpixel S_k at time t, in a given color space (RGB or CIELAB).

Algorithm details

Superpixels are grown sequentially, referring to Fig. 8.

A superpixel area increase from a seed pixel. The seed of the first superpixel can be any pixels in the image, thus we arbitrarily take the center pixel of the image. Starting from a seed, an superpixel grows by adding the eligible neighboring pixels. The growth of superpixels are constrained by the parameter T, provided by the user. When the distances of all the path starting from the seed pixel exceed the threshold T, the growth of superpixel terminates.

A visual description of the process that growing a superpixel refers to Fig. 9. First, seed s is added to superpixel S_k, and the path distance $D_s = 0$, (s, D_s) is added to distance minimum priority queue Q. Second, the superpixel p with the minimum path distance D_p is popped from distance minimum priority queue Q, (p, D_p). If $D_p < T$, the neighbors of p that meet one of the following conditions can be added to superpixel S_k and priority queue Q: for neighbor pixel p_{nb}, (1) p_{nb} is not assigned to any superpixels; (2) p_{nb} is not assigned to superpixels S_k and the new path distance $D_{p_{nb}}$ is smaller than the old path distance of p_{nb}, the new path distance $D_{p_{nb}} = D_p \times \beta + \text{colordis}_{p_{nb}}$. If $D_p >= T$, p is a boundary pixel of superpixel S_k, and the neighbors of p that not assigned to any superpixels are added to seeds set X. Loop through the second step until priority queue Q is empty. Then a new seed s is taken from seed set X. A new superpixel grows from the new seed that not assigned to any superpixels.

An superpixel can claim a pixel from an existing superpixel if its path distance is closer to it. This makes superpixels competing for pixel ownership to ensure

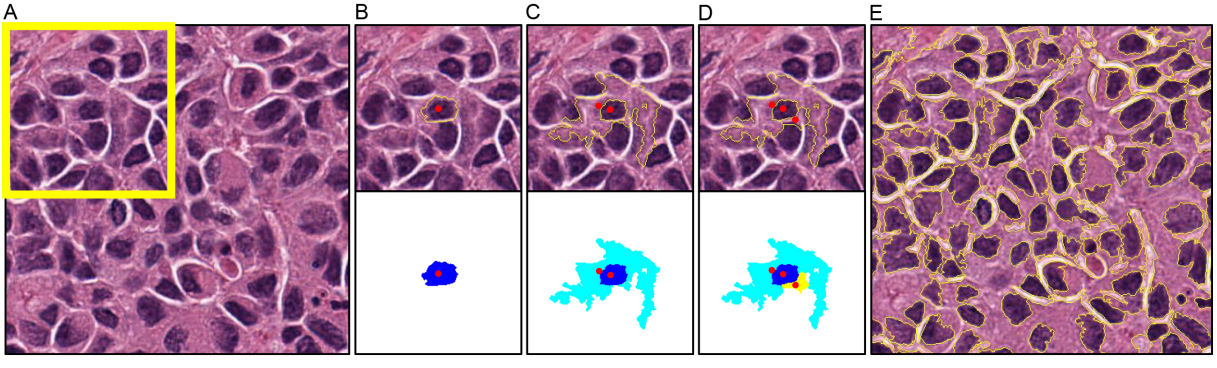

Figure 8. The process of scale-adaptive superpixel segmentation for medical images. (A) A part of an image for computational pathology from dataset [29]. (B) The first superpixel is grown from the seed (red circle), by gathering neighboring pixels, making use of breadth-first search and greedily shortest path strategy. When the distances of all the path starting from the seed pixel exceed the threshold T, the growth of superpixel terminates. (C) and (D) show a new seed (red circle) is picked from the borders of existing superpixels. A superpixel can claim a pixel from an existing superpixel if its path distance is smaller than previous, which encourages boundary adherence. (D) The final superpixel segmentation of (A).

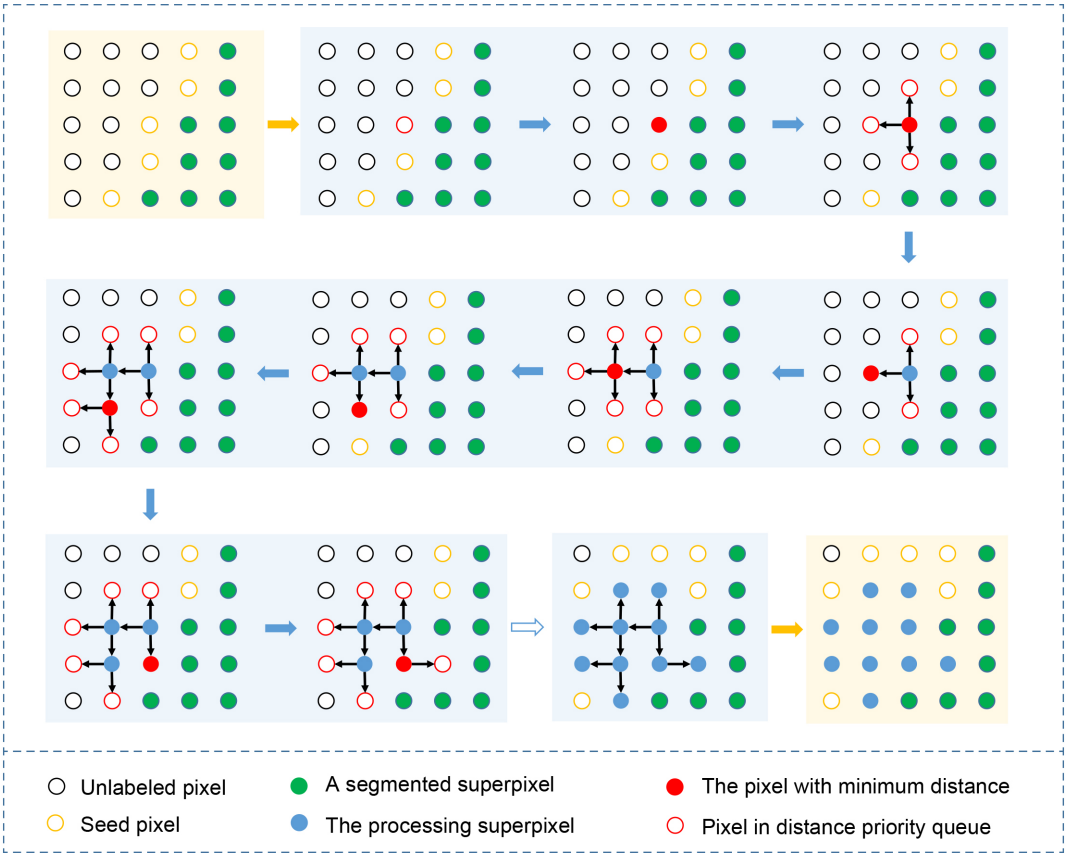

Figure 9. The process of growing a superpixel from a seed pixel.

Algorithm 1: Scale-adaptive superpixels for medical images

Input: Image I, seed pixel s, threshold T and parameter β
Output: Set of superpixels Ω

$\Omega \leftarrow \emptyset$;
Set of seeds $X \leftarrow s$;
while S is not empty **do**
  Get seeds $s \in X$;
  $L_k, X_{new} \leftarrow$ CreateSuperpixel(s, T, β);
  $\Omega \leftarrow \Omega \cup \{L_k\}$;
  $X \leftarrow X \cup X_{new}$;
  Remove seeds from X that are assigned to an superpixel;
return Ω;

Algorithm 2: CreateSuperpixel: Growing an superpixel S_k

Input: Seed pixel s, threshold T and parameter β
Output: The superpixel S_k, new seeds set X_{new}

Initialize superpixel $S_k \leftarrow s$;
Initialize the distance map D: the distance of seed s as 0, all other pixels as ∞;
Set average color C_k^1 to color of s;
Initialize minimum priority queue Q: push s into Q;
while Q is not empty **do**
  Get pixel $p \in Q$ with the smallest distance D_p
  Remove p from
  if $D_p < T$ **then**
    for each neighbor p_{nb} of p **do**
      if $D_p \times \beta +$ colordis$_{p_{nb}} < D_{p_{nb}}$ and label *of* p_{nb} is not k **then**
        $D_{p_{nb}} = D_p \times \beta +$ colordis$_{p_{nb}}$;
        $S_k \leftarrow S_k \cup \{p_{nb}\}$;
        Update C_k with S_k average color;
        push p_{nb} into Q;
  else
    Add neighbors of p to X_{new}
return S_k, X_{new};

better boundary adherence.

The algorithm is presented more formally in Algorithms 1 and 2.

ACKNOWLEDGEMENTS

The work was supported by the NSFC-Zhejiang Joint Fund of the Integration of Informatization and Industrialization (No. U1909210), the National Natural Science Foundation of China (No. 61772312), and the Fundamental Research Funds of Shandong University (No. 2018JC030).

COMPLIANCE WITH ETHICS GUIDELINES

The authors Limin Sun, Dongyang Ma and Yuanfeng Zhou declare that they have no conflict of interest or financial conflicts to disclose. All

procedures performed in studies involving animals were in accordance with the ethical standards of the institution or practice at which the studies were conducted, and with the 1964 Helsinki declaration and its later amendments or comparable ethical standards.

REFERENCES

1. Ren, X. and Malik, J. (2003) Learning a classification model for segmentation. In: 9th IEEE International Conference on Computer Vision (ICCV 2003), pp. 10−17
2. Bharath, H. N., Colleman, S., Sima, D. M. and Huffel, S. V. (2017) Tumor segmentation from multimodal MRI using random forest with superpixel and tensor based feature extraction. In: Brainlesion: Glioma, Multiple Sclerosis, Stroke and Traumatic Brain Injuries–Third International Workshop, Crimi, A., Bakas, S., Kuijf, H. J., Menze, B. H. and Reyes, M. (Eds.), pp. 463−473
3. Li, H., Wei, D., Cao, S., Ma, K., Wang, L. and Zheng, Y. (2020) Superpixel-guided label softening for medical image segmentation. In: Medical Image Computing and Computer Assisted Intervention –MICCAI 2020– 23rd International Conference, Martel, A. L., Abolmaesumi, P., Stoyanov, D., Mateus, D., Zuluaga, M. A., Zhou, S. K., Racoceanu, D. and Joskowicz, L. (Eds.), pp. 227−237
4. Huang, Q., Huang, Y., Luo, Y., Yuan, F. and Li, X. (2020) Segmentation of breast ultrasound image with semantic classification of superpixels. Med. Image Anal., 61, 101657
5. Farag, A., Lu, L., Roth, H. R., Liu, J., Turkbey, E. and Summers, R. M. (2017) A bottom-up approach for pancreas segmentation using cascaded superpixels and (deep) image patch labeling. IEEE Trans. Image Process., 26, 386−399
6. Leblond, A. and Kauffmann, C. (2016) Ultrafast superpixel segmentation of large 3d medical datasets. In: Medical Imaging 2016: Biomedical Applications in Molecular, Structural, and Functional Imaging, Gimi, B. and Kr'ol, A. (Eds.), pp. 97881N
7. Tian, Z., Liu, L., Zhang, Z. and Fei, B. (2016) Superpixel-based segmentation for 3d prostate MR images. IEEE Trans. Med. Imaging, 35, 791−801
8. da Silva, G. L. F., Diniz, P. S., Ferreira, J. L., França, J. V. F., Silva, A. C., de Paiva, A. C. and de Cavalcanti, E. A. A. (2020) Superpixel-based deep convolutional neural networks and active contour model for automatic prostate segmentation on 3D MRI scans. Med. Biol. Eng. Comput., 58, 1947−1964
9. Ouyang, C., Biffi, C., Chen, C., Kart, T., Qiu, H. and Rueckert, D. (2020) Self-supervision with superpixels: Training few-shot medical image segmentation without annotation. In: Computer Vision –ECCV 2020– 16th European Conference, Vedaldi, A., Bischof, H., Brox, T. and Frahm, J. (Eds.), pp. 762–780
10. Nguyen, D. C. T., Benameur, S., Mignotte, M. and Lavoie, F. (2018) Superpixel and multi-atlas based fusion entropic model for the segmentation of x-ray images. Med. Image Anal., 48, 58−74
11. Achanta, R. and Su¨sstrunk, S. (2017) Superpixels and polygons using simple noniterative clustering. In: 2017 IEEE Conference on Computer Vision and Pattern Recognition, CVPR 2017, pp. 4895−4904
12. Liu, M., Tuzel, O., Ramalingam, S. and Chellappa, R. (2011) Entropy rate superpixel segmentation. In: The 24th IEEE Conference on Computer Vision and Pattern Recognition, CVPR 2011, pp. 2097−2104
13. Janowczyk, A. and Madabhushi, A. (2016) Deep learning for digital pathology image analysis: A comprehensive tutorial with selected use cases. J. Pathol. Inform., 7, 29
14. Shi, J. and Malik, J. (2000) Normalized cuts and image segmentation. IEEE Trans. Pattern Anal. Mach. Intell., 22, 888−905
15. Felzenszwalb, P. F. and Huttenlocher, D. P. (2004) Efficient graph-based image segmentation. Int. J. Comput., 59, 167−181
16. Achanta, R., Shaji, A., Smith, K., Lucchi, A., Fua, P. and Süsstrunk, S. (2012) SLIC superpixels compared to state-of-the-art superpixel methods. IEEE Trans. Pattern Anal. Mach. Intell., 34, 2274−2282
17. Levinshtein, A., Stere, A., Kutulakos, K. N., Fleet, D. J., Dickinson, S. J. and Siddiqi, K. (2009) TurboPixels: fast superpixels using geometric flows. IEEE Trans. Pattern Anal. Mach. Intell., 31, 2290−2297
18. Zhou, Y., Pan, X., Wang, W., Yin, Y. and Zhang, C. (2017) Superpixels by bilateral geodesic distance. IEEE Trans. Circ. Syst. Video Tech., 27, 2281−2293
19. den Bergh, M. V., Boix, X., Roig, G., de Capitani, B. and Gool, L. V. (2012) SEEDS: superpixels extracted via energy-driven sampling. In: Computer Vision –ECCV 2012– 12th European Conference on Computer Vision, Fitzgibbon, A. W., Lazebnik, S., Perona, P., Sato, Y. and Schmid, C. (Eds.), pp. 13−26
20. Vincent, L. and Soille, P. (1991) Watersheds in digital spaces: An efficient algorithm based on immersion simulations. IEEE Trans. Pattern Anal. Mach. Intell., 13, 583−598
21. Comaniciu, D. and Meer, P. (2002) Mean shift: A robust approach toward feature space analysis. IEEE Trans. Pattern Anal. Mach. Intell., 24, 603−619
22. Jampani, V., Sun, D., Liu, M., Yang, M. and Kautz, J. (2018) Superpixel sampling networks. In: Computer Vision –ECCV 2018– 15th European Conference, Ferrari, V., Hebert, M., Sminchisescu, C. and Weiss, Y. (Eds.), pp. 363−380
23. Yang, F., Sun, Q., Jin, H. and Zhou, Z. (2020) Superpixel segmentation with fully convolutional networks. In: 2020

IEEE/CVF Conference on Computer Vision and Pattern Recognition, CVPR 2020, pp. 13961−13970
24. Stutz, D., Hermans, A. and Leibe, B. (2018) Superpixels: An evaluation of the stateof-the-art. Comput. Vis. Image Underst., 166, 1−27
25. Achanta, R., Marquez Neila, P., Fua, P. and Süsstrunk, S. (2018) Scale-adaptive superpixels. In: 26th Color and Imaging Conference Final Program and Proceedings, pp. 1−6
26. Uziel, R., Ronen, M. and Freifeld, O. (2019) Bayesian adaptive superpixel segmentation. In: 2019 IEEE/CVF International Conference on Computer Vision, ICCV 2019, pp. 8469−8478
27. Bauchet, J. and Lafarge, F. KIPPI: kinetic polygonal partitioning of images. In: 2018 IEEE Conference on Computer Vision and Pattern Recognition, pp. 3146−3154
28. Ma, D., Zhou, Y., Xin, S. and Wang, W. (2021) Convex and compact superpixels by edge-constrained centroidal power diagram. IEEE Trans. Image Process., 30, 1825−1839
29. Kumar, N., Verma, R., Sharma, S., Bhargava, S., Vahadane, A. and Sethi, A. (2017) A dataset and a technique for generalized nuclear segmentation for computational pathology. IEEE Trans. Med. Imaging, 36, 1550−1560
30. Dataset. https://tianchi.aliyun.com/competition/ (Accessed: January 1, 2021)
31. Shi, F., Yap, P. T., Wu, G., Jia, H., Gilmore, J. H., Lin, W. and Shen, D. (2011) Infant brain atlases from neonates to 1- and 2-year-olds. PLoS One, 6, e18746
32. Wang, J. and Wang, X. (2012) VCells: simple and efficient superpixels using edge-weighted centroidal voronoi tessellations. IEEE Trans. Pattern Anal. Mach. Intell., 34, 1241−1247
33. Neubert, P. and Protzel, P. (2012) Superpixel benchmark and comparison. In: Proc. Forum Bildverarbeitung, Vol. 6
34. Nowozin, S., Gehler, P. V. and Lampert, C. H. (2010) On parameter learning in crfbased approaches to object class image segmentation. In: Computer Vision–ECCV 2010–11th European Conference on Computer Vision, Daniilidis, K., Maragos, P. and Paragios N. (Eds.), pp. 98−111

